Acta Crystallographica Section B
Structural Science
ISSN 0108-7681

Estimation of polyhedral compressibilities and structural evolution of $GdFeO_3$-type perovskites at high pressures

J. Zhao,* N. L. Ross and R. J. Angel

Crystallography Laboratory, Department of Geosciences, Virginia Polytechnic Institute and State University, Blacksburg, VA 24061, USA

Correspondence e-mail: jzhao@vt.edu

Received 29 December 2005
Accepted 13 March 2006

A new approach based on the bond-valence matching relation is developed to predict the detailed structural evolution of $GdFeO_3$-type perovskites at high pressure from knowledge of the room-pressure structure and the high-pressure unit-cell parameters alone. The evolution of perovskite structures estimated in this way is in good agreement with the structure refinements available from high-pressure single-crystal diffraction measurements of a number of perovskites. The method is then extended to predict the structure of $MgSiO_3$ perovskite at pressures for which no single-crystal structural data are available and the results are compared to *ab initio* quantum calculations of $MgSiO_3$ perovskite up to 120 GPa.

1. Introduction

The orthorhombic $GdFeO_3$-type perovskites (space-group symmetry *Pbnm*), with the general stoichiometry ABO_3, are derived from the ideal cubic structure with *Pm*3*m* symmetry *via* the tilting and distortion of BO_6 octahedra (*e.g.* Glazer, 1972; Megaw, 1973; Thomas, 1989; Woodward, 1997*a*; Howard & Stokes, 2005). The pressure-induced evolution of these polyhedra totally determines the trends of structural change and, in turn, determines the variation of physical properties such as energies, electric and magnetic susceptibilities, electric dipolar moments, and elastic wave speeds with pressure (*e.g.* Woodward, 1997*b*; Wentzcovitch *et al.*, 2004; Zhou *et al.*, 2005). The tilts and distortions of the BO_6 octahedra are strongly coupled to the distortion of the AO_{12} coordination polyhedra in orthorhombic perovskite oxides. This coupling then leads to two distinct patterns of behavior of perovskites with increasing pressure that are controlled by the relative compressibilities of the BO_6 and AO_{12} polyhedra. When the AO_{12} polyhedra are more compressible than the BO_6 octahedra, the latter become more tilted and distorted and consequently the AO_{12} polyhedra in turn become more distorted. Examples include $MgSiO_3$, $CaSnO_3$ and $NaMgF_3$ (Ross & Hazen, 1990; Zhao *et al.*, 2004*a*; Liu *et al.*, 2005). In contrast, when the AO_{12} polyhedra are less compressible than the BO_6 octahedra the tilts of the octahedra decrease with increasing pressure and, as a result, the AO_{12} polyhedra become less distorted as well, as in $YAlO_3$ (Ross *et al.*, 2004*a*). Therefore, the relative compressibilities of the BO_6 and AO_{12} polyhedra are the key for understanding the high-pressure behavior and structural stability of ABO_3 perovskites.

High-pressure single-crystal X-ray diffraction has proved to be an effective tool for characterizing atomic level compression mechanisms and structure changes in condensed systems under high pressure, but the technique is mostly applied to studies at pressures of less than 10 GPa because of a number of technical challenges and limitations. These include the

reduction in diffraction signal from the smaller samples required for higher-pressure studies, and the need to load He or H_2 as the pressure medium to ensure hydrostatic conditions above 10 GPa. High-pressure powder X-ray diffraction is a good complement to single-crystal diffraction, especially if there is no single-crystal sample available. However, the lack of a true powder average in the small sample sizes in the diamond–anvil cell, as well as the presence of inter-granular stresses (*e.g.* Takemura, 2001), means that the intensities from high-pressure powder diffraction experiments are normally insufficiently accurate to allow the details of the structural changes such as the compressibilities of bond lengths and tilting of BO_6 octahedra to be determined in perovskites under high pressure. However, unit-cell parameters, which are determined solely by the positions of the diffraction maxima, can be measured with high accuracy in such powder diffraction experiments. Therefore, in order to explore the pressure-induced variation of bond lengths and angles of perovskites at pressures above 10 GPa, it is essential to develop a simple approach to estimate polyhedral compressibilities in perovskites from measurements of the unit-cell parameters alone.

Several methods have been applied to estimate the compression of bond lengths and changes of bond angles under high pressure. Experimentally, Hazen & Finger (1979) developed the general idea that the bulk compressibility of most metal oxides is closely related to the polyhedral compressibility and the linkage of the polyhedra. An empirical relation was established in which the polyhedral compressibilities are proportional to the polyhedral volumes and inversely proportional to the formal charges of the cations and the anions, as well as the empirical iconicity (Hazen & Finger, 1979). Theoretical approaches such as *ab initio* quantum calculations and empirical potential methods have also been widely applied to this purpose (*e.g.* Wentzcovitch *et al.*, 2004; Payne *et al.*, 1992; Magyari-Köpe *et al.*, 2002; Brodholt *et al.*, 2002; Allan, 2004; Iitaka *et al.*, 2005.

Whatever the approach used, the accurate prediction of compressibility requires an accurate description of both the structure and the structural dependence of the interactions between cations and anions. In contrast to *ab initio* models, one simpler approach is that based upon the concept of bond valence (Brown & Altermatt, 1985; Brese & O'Keeffe, 1991; Brown, 1992, 2001), in which the valence (or strength, s_i) of an individual bond is given by

$$s_i = \exp\left(\frac{R_0 - R_{ij}}{B}\right), \quad (1)$$

in which R_{ij} is the bond length between cation i and anion j, R_0 is a constant specific to any pair of anion and cation, and B = 0.37 Å is a universal constant (Brown & Altermatt, 1985; Brese & O'Keeffe, 1991). In stable structures at room pressure, the sum of the valences of all of the bonds to any cation in the structure is equal to its formal valence, V_i

$$V_i = \sum_j^N \exp\left(\frac{R_0 - R_{ij}}{B}\right), \quad (2)$$

where N is the coordination number. We then proposed that the pressure-induced changes in the bond-valence sums V_i at the two cation sites within any given perovskite are equal ($\Delta V_A = \Delta V_B$) (Zhao *et al.*, 2004*b*), and this has been confirmed by a series of high-pressure single-crystal X-ray diffraction measurements. Given this match of evolution of bond valences with pressure one can show that the ratio of cation-site compressibilities is estimated by $\beta_B/\beta_A = M_A/M_B$ (Zhao *et al.*, 2004*b*), in which the site parameter M_i is defined in terms of the average bond length (R_i) at room pressure

$$M_i = (R_i N/B)\exp[(R_0 - R_i)/B]. \quad (3)$$

The parameter M_i thus represents the variation of the bond-valence sum at the central cation in a polyhedral site due to the change of the average bond distance R_i. By calculating M_A/M_B from crystal structure data at room pressure we can therefore estimate the relative compressibilities of AO_{12} and BO_6 polyhedra and thus predict the general evolution of the perovskite structure with increasing pressure. In general, in perovskites with a cation of formal charge +2 in the A site, and a B cation with a formal charge of +4, $M_A/M_B = \beta_B/\beta_A < 1$ and the structures will become more distorted, or transform to structures of lower symmetry (*e.g.* Zhao *et al.*, 2004*a*; Angel, Zhao & Ross, 2005). The same is true for fluoride perovskites such as $NaMgF_3$ (Liu *et al.*, 2005). When both A and B cations have formal charges of +3, $M_A/M_B = \beta_B/\beta_A$ is generally greater than unity, and pressure thus induces a decrease of octahedral tilting and/or transitions to structures of higher symmetry (Angel, Zhao & Ross, 2005).

The concept of bond-valence matching between the A and B cation sites of perovskites thus provides a simple and universal basis for predicting the dominant mechanism or the coupling relation that governs the pressure-induced octahedral tilts and distortions in both sites. However, the relationship $\beta_B/\beta_A = M_A/M_B$ clearly only predicts the relative compressibilities of the two sites and does not predict the absolute values. Thus, it cannot be used to predict the exact bond lengths and angles of a perovskite at high pressure unless the empirical correlations between the site-compressibility ratio M_A/M_B and the rate of octahedral tilting measured in high-pressure single-crystal diffraction experiments are considered (*e.g.* Angel, Zhao & Ross, 2005). In this paper we use the bond-valence matching principle to predict the detailed structures of perovskites at high pressures from room-pressure crystal structure data and only the unit-cell parameters of the perovskites at high pressure. This allows structural information to be obtained from high-pressure experiments in which only the unit-cell parameters have been reliably determined. The method is applied to 2:4-type perovskites Ca(Zr, Sn, Ti, Ge)O_3 and some 3:3-type perovskites ($YAlO_3$, $GdAlO_3$ *etc.*) and the predictions are compared to the results from high-pressure single-crystal diffraction measurements. Finally, we use the method to predict the structure of $MgSiO_3$ perovskite at pressures for which no single-crystal structural data are available.

2. Theory

The tilting of the octahedra in an orthorhombic perovskite can be characterized by the two symmetry-independent bond angles $B-O1-B$ and $B-O2-B$. The changes in these two angles with pressure, denoted below as α_i (i = 1,2), are approximately determined by the average compressibilities of the B site and the unit-cell parameters (Ross *et al.*, 2004*a*; Zhao *et al.*, 2004*a*)

$$\alpha_i = 2\sin^{-1}[\exp(\Delta\beta_i P)\sin(\alpha_{0,i}/2)] \tag{4}$$

where $\Delta\beta_1 = \beta_{B-O1} - \beta_c$, $\Delta\beta_2 = \beta_{B-O2} - \beta_{ab}$ and $\beta_{ab} = (a^2\beta_a + b^2\beta_b)/(a^2 + b^2)$, $\alpha_{0,i}$ are the bond angles $B-Oi-B$ at room pressure and β_a, β_b, β_c are the linear compressibilities of the unit-cell parameters. Given that the distortion of the BO_6 octahedra changes very little with pressure, the average bond compressibility β_B is a good approximation in place of the individual bond compressibilities β_{B-O1} and β_{B-O2}.

In order to determine the changes in the $B-O-B$ bond angles from (4) we therefore need the evolution of the unit-cell parameters with pressure, as well as the average compressibility of the $B-O$ bond lengths. The former can be obtained from high-pressure powder diffraction experiments, while the latter can be related to the variation of the bond-valence sum with pressure [by differentiation of (2) and taking averages]

$$\beta_B = -\frac{1}{R_{0,B}}\frac{dR_B}{dP} = \frac{B}{R_{0,B}}\frac{d\ln V_B}{dP}, \tag{5}$$

where $R_{0,B}$ is the average bond length of $B-O$ bond at room pressure.

As we show in the following, the bond-valence matching principle allows us to obtain the absolute variation of the bond-valence sum at the B cation site from any reasonable model of the structure that approximates the true structure. In order to prove this assertion, we first note that the stability of perovskites can be described with the concept called the global instability index *GII* (Rao *et al.*, 1998; Salinas-Sanchez *et al.*, 1992; Brown, 2001; Lufaso & Woodward, 2001). At room pressure the structural stability can be estimated by comparing the calculated bond-valence sums with the ideal formal valence through *GII* and the stable structure usually corresponds to a minimum of the *GII*. This suggests that any deviation from the stable or equilibrium configuration would result in higher strains among the bonds (Brown, 2001). This concept can be naturally extended to describe the stability of crystal structure under high pressure. First, the application of pressure results in shorter bonds and both bond-valence strains and an increase in the *GII* compared with the value for the room-pressure structure. Nonetheless, we will assume that the actual structure stable at any given pressure represents a minimum of *GII* with respect to changes in the fractional coordinates of the atoms within the unit cell.

For the purposes of predicting the structure of perovskites, in which the bond-valence matching principle applies, we introduce a local instability index *LII* that is derived from the bond valence sums at the cation sites alone

$$LII = \left[\frac{(\Delta V_A)^2 + (\Delta V_B)^2}{2}\right]^{1/2}, \tag{6}$$

where $\Delta V_A = V_A(x_j^m) - V_A^0(x_j^0)$ and $\Delta V_B = V_B(x_j^m) - V_B^0(x_j^0)$. $V_i(x_i^m)$ and $V_i^0(x_i^0)$ are bond-valence sums at the cation sites for the fractional atomic coordinates of a model structure $\{x_j^m(P)\}$ at pressure P and the room-pressure structure $\{x_j^0(0)\}$ at ambient pressure. The *LII* so defined therefore represents the increase of bond-valence sums in a model structure at high pressure compared with that in the stable observed structure at room pressure. We will further assume that the real configuration of the structure at pressure, represented by the coordinate set $\{x_j^r(P)\}$, is the one in which both the *LII* is a minimum with respect to changes in the fractional coordinates $\{x_j^m(P)\}$ and the bond-matching relation is satisfied. That is, the fractional coordinates of the stable structure at pressure $\{x_j^r(P)\}$ will satisfy the two equations

$$\Delta V_A(x_j^r) = \Delta V_B(x_j^r) \tag{7}$$

$$\left(\frac{\partial LII^2}{\partial x_i^m}\right)_{P,x_j^r} = 0. \tag{8}$$

From (6), (7) and (8), we can obtain for any model structure at pressure

$$\frac{\partial LII^2}{\partial x_j^m} = [V_a(x_j^m) - V_A^0(x_j^0)]\frac{\partial V_A}{dx_j^m} + [V_B(x_j^m) - V_B^0(x_j^0)]\frac{\partial V_B}{dx_j^m}. \tag{9}$$

For the real stable structure at pressure $\{x_j^r(P)\}$, (9) is equivalent to

$$\begin{aligned}\left(\frac{\partial LII^2}{\partial x_i^m}\right)_{P,x_j^r} &= \left[V_A(x_j^r) - V_A^0(x_j^0)\right]\left[\frac{\partial V_A}{\partial x_j^m} + \frac{\partial V_B}{\partial x_j^m}\right]_{P,x_j^r} \\ &= 2\left[V_A(x_j^r) - V_A^0(x_j^0)\right]\left[\frac{\partial[(V_A + V_B)/2]}{\partial x_j^m}\right]_{P,x_j^r} \\ &= 2\left[V_A(x_j^r) - V_A^0(x_j^0)\right]\left[\frac{\partial V_{\rm avg}(x_j^m)}{\partial x_j^m}\right]_{P,x_j^r} = 0,\end{aligned} \tag{10}$$

where $V_{\rm avg}(x_j^m) = [V_A(x_j^m) + V_B(x_j^m)]/2$. In order for this to hold for a high-pressure structure then

$$\left[\frac{\partial V_A}{\partial x_j^m} + \frac{\partial V_B}{\partial x_j^m}\right]_{P,x_j^r} = 0 \text{ which is equivalent to}$$

$$\left[\frac{\partial V_{\rm avg}(x_j^m)}{\partial x_j^m}\right]_{P,x_j^r} = 0. \tag{11}$$

In general, the average bond-valence sum for a model structure $\{x_j^m(P)\}$ can be expanded as

$$\Delta V_{\rm avg}(x_j^m) = \Delta V_{\rm avg}(x_j^r) + \sum_j \left.\frac{\partial \Delta V_{\rm avg}(x_j^m)}{\partial x_j^m}\right|_{P,x_j^r} (x_j^m - x_j^r) + \frac{1}{2}\sum_{j,k} \left.\frac{\partial^2 \Delta V_{\rm avg}(x_j^m)}{\partial x_j^m \partial x_k^m}\right|_{P,x_j^r} (x_j^m - x_j^r)(x_k^m - x_k^r) + \cdots, \quad (12)$$

where $\Delta V_{\rm avg}(x_j^r) = \Delta V_A(x_j^r) = \Delta V_B(x_j^r)$. According to (11), the first summation term in (12) is equal to zero. We thus obtain

$$\Delta V_i(x_j^r) = \Delta V_{\rm avg}(x_j^m) - \tfrac{1}{2}\sum_{j,k} \frac{\partial^2 \Delta V_{\rm avg}(x_j^m)}{\partial x_j^m \partial x_k^m}|_{P,x_j^r} \times (x_j^m - x_j^r)(x_k^m - x_k^r) + \cdots. \quad (13)$$

This equation expresses the result that the true increase of the bond-valence sum $\Delta V_i(x_j^r)$ in the real structure can be approximated by the average bond valence $\Delta V_{\rm avg}(x_j^m)$ of any model structure, provided that the summation term in (13) is small. Estimates of the magnitude of this summation term can be obtained by direct calculation from real and model structures. The pressure-induced variation of the fractional atomic coordinates $\{\Delta x_j = x_j^0 - x_j^r,\ j = 1, 2\cdots\}$ is actually very small. For example, the magnitude of the variation of $\{\Delta x_j\}$ is *ca* 0.001 below 10 GPa for $YAlO_3$ and $CaSnO_3$ (Ross *et al.*, 2004*a*; Zhao *et al.*, 2004*a*), and from *ab initio* calculations of $MgSiO_3$ perovskite (Wentzcovitch *et al.*, 1995) the magnitude of variation is *ca* 0.01 up to 100 GPa. Variations in the coordinates of a model structure (x_j^m) cannot exceed these values without resulting in a structure other than perovskite, so the coordinate terms in (13) are therefore of the order of less than 10^{-4}. We also find that the derivative term $\partial^2 \Delta V_{\rm avg}/\partial x_j^{m2}$ changes by less than 0.001 for individual coordinate changes of up to *ca* $\pm$ 20% in the rigid-octahedra model (discussed in detail later), which is actually larger than the entire variation from room pressure to 100 GPa for $MgSiO_3$ perovskite (Wentzcovitch *et al.*, 1995). This result can be easily understood in terms of the structure. Any shift of an O-atom position will have the opposite effects on the A—O and B—O bond lengths, resulting in an increase in one bond-valence sum and a decrease in the other, and only a much smaller change in the average of the two. As the A cation is bonded on all sides, any shift in its position will shorten some A—O bonds and lengthen others, so to first order the bond-valence sum will again be unchanged. The B cation occupies a special position in *Pbnm* perovskites and cannot be shifted.

Therefore, (13) expresses the result that the real bond-valence sums of the equilibrium structure of a perovskite at high pressure are well approximated by the average bond-valence increase, $\Delta V_{\rm avg}(x_j^m)$, of any reasonable model structure with the same unit-cell parameters as the real structure. The real structural changes in perovskites under compression are known to involve both compression and rotation of the BO_6 octahedra. However, we can consider these two mechanisms separately in order to derive two extreme models of the evolution of the perovskite structure with pressure, with the knowledge that the real structural evolution will fall between these two extremes.

In the rigid-octahedra model, the fractional coordinates are adjusted so that the B—O bond lengths and O—B—O bond angles remain constant, and the compression is accommodated entirely by rotation of the octahedra and consequent reduction of the B—O—B bond angles. The bond-valence sum at the B cation site then remains unchanged at its room-pressure value, while the bond-valence sum at the A-cation

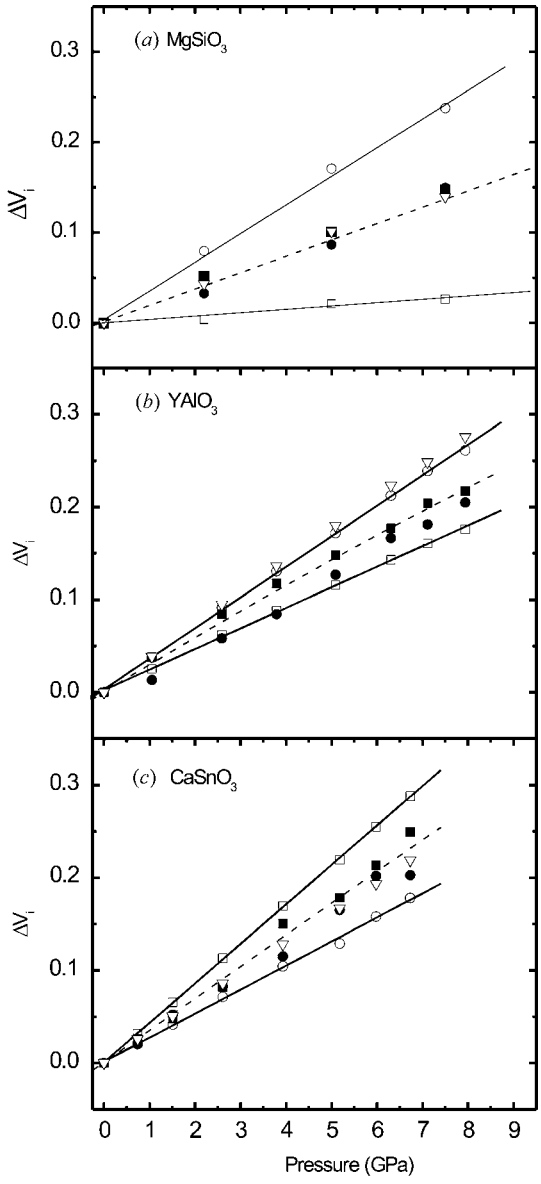

Figure 1
A comparison of the experimentally observed evolution of the bond-valence sums at the A and B cation sites in perovskites with that predicted by models. Bond-valence sums for the A sites are shown as circles and the B sites as squares, throughout. The solid symbols represent sums calculated from experimental data and the open symbols are the sums predicted from the unit-cell parameters for various models. The mean of the rigid-octahedra model (open triangles) provides a good estimate of the experimental data for $MgSiO_3$ and $CaSnO_3$, but does not for $YAlO_3$ in part (*b*) because of the direction of octahedral tilting in the latter. The *fixed-coordinate* model provides better estimates (dashed lines) of the true evolution of the structure for all perovskites.

Table 1
Comparison between predictions and experiments.

Perovskite *Pbnm*	M_A/M_B^k	$d\ln V/dP$	β_{BO6} prediction $\times 10^{-3}$ GPa^{-1}	β_{BO6} experiment $\times 10^{-3}$ GPa^{-1}	β_{AO12} prediction $\times 10^{-3}$ GPa^{-1}	β_{AO12} experiment $\times 10^{-3}$ GPa^{-1}	β_{AO8} experiment $\times 10^{-3}$ GPa^{-1}	β_{AO4} experiment $\times 10^{-3}$ GPa^{-1}	β_{AO12} calculated by (17) $\times 10^{-3}$ GPa^{-1}
$GdAlO_3$[a]	1.33	0.00938 (12)	1.82 (6)	1.71 (11)	1.37 (6)	1.60 (24)	0.99 (27)	2.83 (20)	1.45
$YAlO_3$[b]	1.32	0.00967 (14)	1.87 (7)	1.72 (10)	1.42 (7)	1.57 (2)	1.11 (9)	2.45 (15)	1.41
$Gd_{0.80}Nd_{0.20}AlO_3$[c]	1.33	0.00996 (10)	1.93 (5)	1.87 (13)	1.46 (5)	1.71 (11)	1.05 (8)	3.03 (13)	1.55
$LaGaO_3$[d]	1.22	0.01134 (12)	2.12 (6)	2.43 (7)	1.59 (6)	2.07 (3)	0.35 (13)	5.0 (3)	1.82
$NdGaO_3$[d]	1.18	0.01037 (27)	1.94 (7)	1.81 (7)	1.64 (7)	1.68 (17)	1.05 (18)	2.95 (14)	1.54
$GdFeO_3$[a]	1.15	0.00973 (14)	1.79 (7)	1.75 (13)	1.56 (7)	1.63 (12)	1.5 (1)	1.9 (1)	1.51
$ScAlO_3$[e]	1.06	0.00798 (32)	1.55 (17)	1.62 (9)	1.46 (17)	1.45 (2)	1.49 (2)	1.38 (3)	1.42
$CaZrO_3$[f]	0.53	0.00842 (16)	1.49 (7)	–	2.81 (7)	–	–	–	1.87
$CaSnO_3$[g]	0.56	0.00835 (25)	1.50 (12)	1.61 (11)	2.67 (12)	1.84 (23)	2.23 (29)	1.05 (12)	1.92
$CaTiO_3$[h]	0.63	0.00729 (17)	1.38 (9)	1.48 (12)	2.19 (9)	1.66 (24)	1.96 (27)	1.07 (19)	1.68
$CaGeO_3$[i]	0.75	0.00690 (11)	1.35 (6)	–	1.80 (6)	–	–	–	1.52
$MgSiO_3$[j]	0.70	0.00419 (6)	0.87 (3)	0.86 (13)	1.22 (3)	1.06 (4)	1.44 (9)	0.67 (23)	1.22

References: (*a*) Ross *et al.* (2004*b*), Ross, Zhao, Burt & Chapuis (2004); (*b*) Ross *et al.* (2004*a*); (*c*) N. L. Ross *et al.*, unpublished; (*d*) J. Zhao *et al.*, unpublished; Berkowski *et al.* (2000); (*e*) Ross (1998); (*f*) Koopmans *et al.* (1983); Ross & Chaplin (2003); (*g*) Zhao *et al.* (2004*a*), Kung *et al.* (2001); (*h*) Ross & Angel (1999), Sasaki *et al.* (1987); (*i*) Sasaki *et al.* (1983); (*j*) Ross & Hazen (1990); (*k*) Zhao *et al.* (2004*b*).

site will increase more rapidly than in the real structure as the A—O bonds become shorter as a result of the octahedral rotations. In practice, distance–least-squares simulations of the perovskite structure with the *DLS*-76 program (Baerlocher *et al.*, 1976) indicate that for most perovskites, octahedra with the internal bond lengths and angles found at room pressure cannot be accommodated within the experimentally measured unit cell at high pressures. This, of course, is consistent with the experimental measurement of significant compression in the octahedra of perovskites. Thus, the DLS simulations actually provide a model structure with the minimum amount of compression of the octahedra or most rigid octahedra that would be consistent with the observed unit-cell compression. The increase in the bond-valence sum at the B cation site, $\Delta V_B(x_j^m)$, is then much less than experimentally observed, but the increase in $\Delta V_A(x_j^m)$ is much larger and consequently the average of these two $\Delta V_{\rm avg}(x_j^m)$ matches the evolution of the bond-valence sums of, for example, $MgSiO_3$ measured experimentally (Fig. 1*a*). For the rigid octahedra model of 2:4 (or 1:2) perovskites the summation term

$$\sum_{j,k} \left.\frac{\partial^2 \Delta V_{\rm avg}(x_j^m)}{\partial x_j^m \partial x_k^m}\right|_{P,x_j^r} (x_j^m - x_j^r)(x_k^m - x_k^r)$$

in (13) is quite small, for example, *ca* 0.01 for $CaSnO_3$ at 7.6 GPa. Thus, the rigid-octahedra model provides a good estimate of the real behavior of such structures because it mimics the low octahedral compressibility and increase in tilting with pressure that is observed experimentally. By contrast, while the rigid-octahedral model of 3:3 perovskites also exhibits increased octahedral tilts with pressure, the real structures exhibit the opposite trend because the octahedra are more compressible than the A-cation site. As a consequence, for 3:3 perovskites the average bond-valence increase predicted by the model (*e.g.* ~ 0.05 for $YAlO_3$ at 7.9 GPa in Fig. 1*b*) does not approximate the experimental data so well.

The other extreme model for a perovskite is one in which all of the compression is accommodated by octahedral compression, with no rotation of the octahedra. This is a much more difficult model to generate in the general case, but the relative isotropy of compression of the unit-cell parameters of most perovskites means that it can be approximated by a model in which the fractional coordinates of all of the atoms remain fixed at their room-pressure values. We therefore term this the 'fixed coordinate' or '*f-c*' model. For 2:4 perovskites this model provides as good an estimate of the evolution of the average bond-valence sums as the rigid-octahedra model (Figs. 1*a* and *c*). Further, because the model mimics the true behavior of the 3:3 perovskites more closely than the rigid-octahedra model, and thus leads to smaller summation terms in (13), it also provides a good estimate of the behavior of these at high pressure (*e.g.* Figs. 1*b* and *c*).

3. Results

We have shown that both the *f-c* model and the rigid-octahedra model provide reasonably accurate estimates of the evolution of the bond-valence sums $\Delta V_{\rm avg}(x_j^r) = \Delta V_A(x_j^r) = \Delta V_B(x_j^r)$ in the actual structures of perovskites at high pressure. As the *f-c* model requires less computation to construct than that with rigid octahedra we will use it in this section to estimate $\Delta V_{\rm avg}(x_j^r)$ and thus the changes in bond lengths and angles in perovskites at high pressures through (4) and (5).

As a test of this approach, the compressibilities of the BO_6 octahedra were predicted for a number of perovskites for which we have high-pressure structures refined from single-crystal X-ray diffraction data to pressures of up to 10 GPa. The resulting values of β_B (Table 1) are generally in good agreement with the direct measurements, with most predicted values falling within 2 e.s.d.s of the measured values. Estimates of the average compressibility of the A site obtained through the relationship $\beta_A = \beta_B/(M_A/M_B)$ however show a poorer agreement with experimental values (Table 1). This is because

our prediction implicitly assumes that all of the $A-O$ distances exhibit the same individual bond compressibility. In contrast, experimental data show that the average bond compressibility, β_{AO8}, of the eight shortest distances in the AO_{12} site, is different from the average compressibility, β_{AO4}, of the four longer $A-O$ distances. As the value of β_{AO4} is closely related to changes in the tilts of the octahedra, it is less than β_{AO8} for 2:4 perovskites, whereas for 3:3 perovskites, $\beta_{AO4} > \beta_{AO8}$ (Zhao *et al.*, 2004*b*). Thus, we find that the estimated β_A is in better agreement with the measured value $\beta_{AO12} = (2\beta_{AO8} + \beta_{AO4})/3$ when the values of β_{AO8} and β_{AO4} are similar, or the ratio M_A/M_B is close to unity, as is the case for $ScAlO_3$ (Table 1).

The *f-c* model provides an alternative method that allows more accurate estimates of β_A to be calculated once β_B is obtained from the model, as follows. The evolution of the true structure from room pressure to high pressure can be described in two steps. First, the unit-cell is compressed while the fractional coordinates of all the atoms remains fixed, so as to generate the *f-c* model structure at pressure. Then, the coordinates are adjusted within the fixed unit cell from the *f-c* model structure so as to obtain the true structure at high pressure. As noted above, the compression of the *f-c* model structure in the first step is accompanied by almost no octahedral rotation. For example, in $CaSnO_3$ from 0 to 6.73 GPa the $B-O_{1,2}-B$ angles of the *f-c* model are unchanged and a similar case can be found in $YAlO_3$. Even when using unit-cell parameters from *ab initio* quantum calculations at 120 GPa, 0 K (Iitaka *et al.*, 2005) and room-pressure crystal structure data (Ross & Hazen, 1990; Vanpeteghem *et al.*, 2006), the calculated $Si-O_{1,2}-Si$ angles of the *f-c* model for $MgSiO_3$ are 146.8 and 147.1°, respectively, very close to the angles 146.4 (3) and 147.5 (2)° measured at room pressure (Ross & Hazen, 1990; Vanpeteghem *et al.*, 2006). We therefore conclude that the majority of the pressure-induced tilting of the octahedra arises from the adjustment of the fractional coordinates, in the second step of the evolution of the structure.

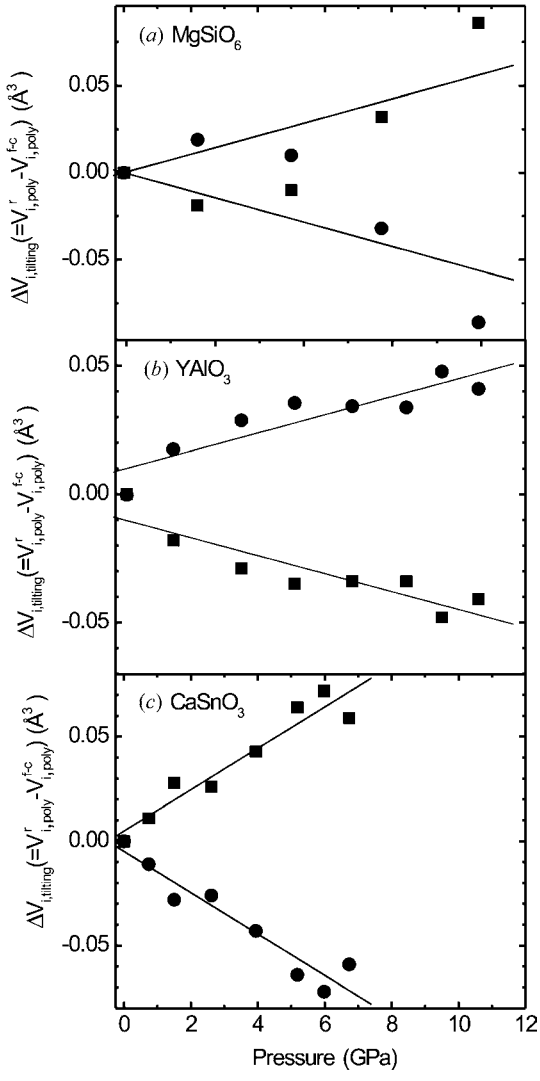

Figure 2
Estimates of the polyhedral volume changes in the *A* and *B* sites that arise from the coordinate shifts from the *fixed coordinate* structure to the true structure for three perovskites. Note that the volume changes increase in magnitude with increasing pressure.

Given these two steps, we can then write the total volume change of a polyhedron from room pressure to the actual structure at high pressure as being the sum of the individual volume changes from the two steps

$$\Delta V_{i,\mathrm{poly}} = \Delta V^{f-c}_{i,\mathrm{poly}} + \Delta V_{i,\mathrm{tilting}}, \qquad (14)$$

where i represents polyhedral AO_{12} or BO_6 and $\Delta V_{i,\mathrm{tilting}}$ is the volume change arising from the shift in coordinates from the *f-c* model to the true structure at constant cell parameters. We denote this as 'tilting' because the resulting changes in the structure are dominated in practice by rotation of the octahedra, but it should be borne in mind that there is also a small component of compression of the octahedra. The sign of $\Delta V_{i,\mathrm{tilting}}$ depends on i and whether BO_6 tilting increases or decreases with pressure. For $MgSiO_3$, $YAlO_3$ and $CaSnO_3$ perovskites as examples, $\Delta V_{i,\mathrm{tilting}}$ is plotted in Fig. 2. Compared with $YAlO_3$ and $CaSnO_3$ (Fig. 2*b* and *c*), we notice that the data for $MgSiO_3$ (Fig. 2*a*) exhibit higher scatter, especially at lower pressures. This is because $Si-O$ bonds are much stiffer than $Al-O$ or $Sn-O$ bonds and thus changes in $Si-O$ bond lengths are of the order of the uncertainty of measurements. However, the general trend of $\Delta V_{i,\mathrm{tilting}}$ is similar to that for $CaSnO_3$.

When the structure is considered as being compressed by changes in the unit-cell parameters alone, with the fractional coordinates fixed, the compressibility of the polyhedra (or any other volume within the structure) must by definition be equal to the compressibility of the unit cell. Thus, differentiation of (14) leads to an expression for the compressibility $\beta_{i,\mathrm{poly}}$ of the AO_{12} and BO_6 polyhedra in terms of the contributions of unit-cell compression and tilting of BO_6 octahedra

$$\beta_{i,\mathrm{poly}} = \beta_{\mathrm{unit\ cell}} + \beta_{i,\mathrm{tilting}}, \qquad (15)$$

where $\beta_{i,\mathrm{tilting}} = -(1/V_{i,\mathrm{poly}})(\Delta V_{i,\mathrm{tilting}}/\Delta P)$ is the component of compressibility owing to the shift in coordinates from the *f-c*

model to the actual structure. As this shift in coordinates is performed with constant unit-cell parameters, and because the AO_{12} and BO_6 polyhedra completely fill the unit-cell volume, we can also write $\Delta V_{A,\text{tilting}} + \Delta V_{B,\text{tilting}} = 0$ and thus

$$V_{A,\text{poly}}/V_{B,\text{poly}} = -\beta_{B,\text{tilting}}/\beta_{A,\text{tilting}}. \quad (16)$$

Thus, (15) and (16) provide another way to calculate the average volume compressibility of the AO_{12} site from the volume compressibility $\beta_{B,\text{poly}} \simeq 3\beta_B$ obtained from the bond-valence matching principle in (3) and the known compressibility of the unit-cell parameters

$$\beta_{A,\text{poly}} = (1 + V_{B,\text{poly}}/V_{A,\text{poly}})\beta_{\text{unit cell}} - (V_{B,\text{poly}}/V_{A,\text{poly}})\beta_{B,\text{poly}}. \quad (17)$$

The resulting values of the average linear compressibilities of the $A-$O bonds, $\beta_A \simeq \beta_{A,\text{poly}}/3$, listed in the last column of Table 1, are more accurate than those calculated from (12), but require no additional input data over that required for the earlier estimates made above.

The variation of the tilting angles with pressure of a series of perovskites with Ca on the A site (*i.e.* CaBO$_3$ with B = Ge, Ti, Sn and Zr) have been predicted from the *f-c* model and (13), (5) and (4), and are compared with experimental data for $CaSnO_3$ and $CaTiO_3$ in Fig. 3. The estimated evolution of the tilting angles with pressure is consistent with experimental results within the uncertainty of the measurements for $CaTiO_3$ (unpublished data) and $CaSnO_3$ (Zhao *et al.*, 2004*a*) perovskites. For $CaGeO_3$ and $CaZrO_3$ perovskite, there are no high-pressure crystal structure data reported yet. The predicted rate of change of the average tilt angles with pressure, $d\langle\alpha_i\rangle/dP$, are -0.096 ($CaGeO_3$), -0.131 ($CaTiO_3$), -0.148 ($CaSnO_3$) and -0.142° GPa^{-1} ($CaZrO_3$), which follows the previously reported trend of decreasing magnitude of $d\langle\alpha_i\rangle/dP$ as the ratio M_A/M_B approaches unity (Zhao *et al.*, 2004*b*). However, we notice that $d\langle\alpha_i\rangle/dP$ for $CaZrO_3$ is predicted to be very similar to that of $CaSnO_3$, in addition to their bond compressibilities being predicted to be very similar (Table 1). This implies that some saturation of pressure-induced variation of structure appears in $CaZrO_3$ as a result of the large tilt angles present in the room-pressure structure as suggested by Ross & Angel (1999).

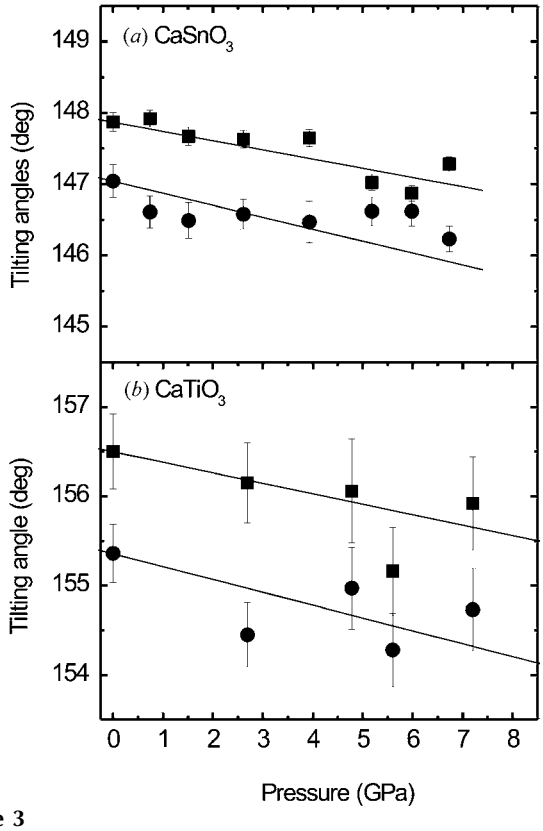

Figure 3
The tilting angles in perovskites as a function of pressure, as indicated by two symmetry-independent bond angles. The predictions of the *fixed coordinate* model, solid lines, are in good agreement with the experimental data shown as solid symbols. Circles are the $B-$O1$-B$ angles, squares are the $B-$O2$-B$ angles.

Owing to its interest in earth science as the major mineral in the Earth's lower mantle, diffraction data and *ab initio* computer simulations of $MgSiO_3$ perovskite extend to much higher pressures than for any other perovskites and can thus provide a more stringent test of both the bond-valence matching principle and the predictive model for the structure. For example, the *ab initio* simulation of $MgSiO_3$ perovskite at 120 GPa (Iitaka *et al.*, 2005) has bond-valence sums at the cation sites of $V_{Si} = 5.60$ v.u. and $V_{Mg} = 4.13$ v.u. Their increase over the values at room pressure are approximately equal, that is, $\Delta V_{Mg}[= V_{Mg}(120) - V_{Mg}(0) = 4.13–2.31\ ] = 1.82$ v.u. and $\Delta V_{Si}\ [= V_{Si}(120) - V_{Si}(0) = 5.60–3.81] = 1.79$ v.u., where bond-valence sums $V_i(0)$ at room pressure are calculated using single-crystal structure data (Ross & Hazen, 1990; Vanpeteghem *et al.*, 2006). Thus, the *ab initio* quantum calculation at 120 GPa is in agreement with the bond-valence matching relation. Fig. 4(*a*) displays the variation of the bond-valence sum $\ln V_i$ of $MgSiO_3$ predicted from the unit-cell parameters measured up to 52 GPa (Ross & Hazen, 1990; Fiquet *et al.*, 2000, Vanpeteghem *et al.*, 2006). For pressures above 10 GPa, note that a quadratic curve represents the evolution of V_i with pressure much better than a straight line, similar to the case of $CaSiO_3$ perovskite (Angel, Ross & Zhao, 2005). The bond-valence sums $\ln V_B$ calculated from *ab initio* quantum calculations (Wentzcovitch *et al.*, 2004; Iitaka *et al.*, 2005; Tsuchiya *et al.*, 2004) are also plotted in Fig. 4(*a*) and are consistent with the extrapolation of the predictions from the experimental data. The compression of the average Si$-$O bond length of $MgSiO_3$ perovskite (Fig. 4*b*), estimated from the bond-valence sum, is in good agreement with both high-pressure single-crystal X-ray diffraction data below 10 GPa (Ross & Hazen, 1990; Vanpeteghem *et al.*, 2006) and *ab initio* simulations at higher pressures (Wentzcovitch *et al.*, 1995; Iitaka *et al.*, 2005; Tsuchiya *et al.*, 2004).

The two tilting angles Si$-$O$_{1,2}-$Si of $MgSiO_3$ perovskite with pressure are estimated through (4) for pressures up to 120 GPa and shown in Figs. 4(*c*) and (*d*), and show a decrease (*i.e.* an increase in tilting) with increasing pressure. Note that the use of linear compressibilities in (4) is usually a good approximation for structures at modest pressures, as for the

calcium oxide perovskites below 10 GPa that we discussed above. However, at higher pressures the compression of unit-cell parameters and bond lengths will depart from linearity with pressure. Therefore, the uncertainties in the predicted tilting angles are expected to be larger. These uncertainties can be estimated by consideration of the uncertainty of β_B ($\Delta\beta_B = \pm 0.03 \times 10^{-3}$ GPa^{-1}, see Table 1), obtained by the linear fit to the variation of the average Si—O bond length with pressure. In Figs. 4(*c*) and (*d*), the gray areas suggest the possible ranges of predicted tilting angles due to the assumption of linear compression of both bonds and unit-cell parameters. The values of the Si—O2—Si angle refined from high-pressure powder X-ray diffraction (Fiquet *et al.*, 2000) agree with the predicted values within the mutual uncertainties (Fig. 4*d*). Note that the bond angles from the *ab initio* simulations underestimate the experimental values at all pressures, but the rates of change of angles with pressure from the simulations agree with our predictions.

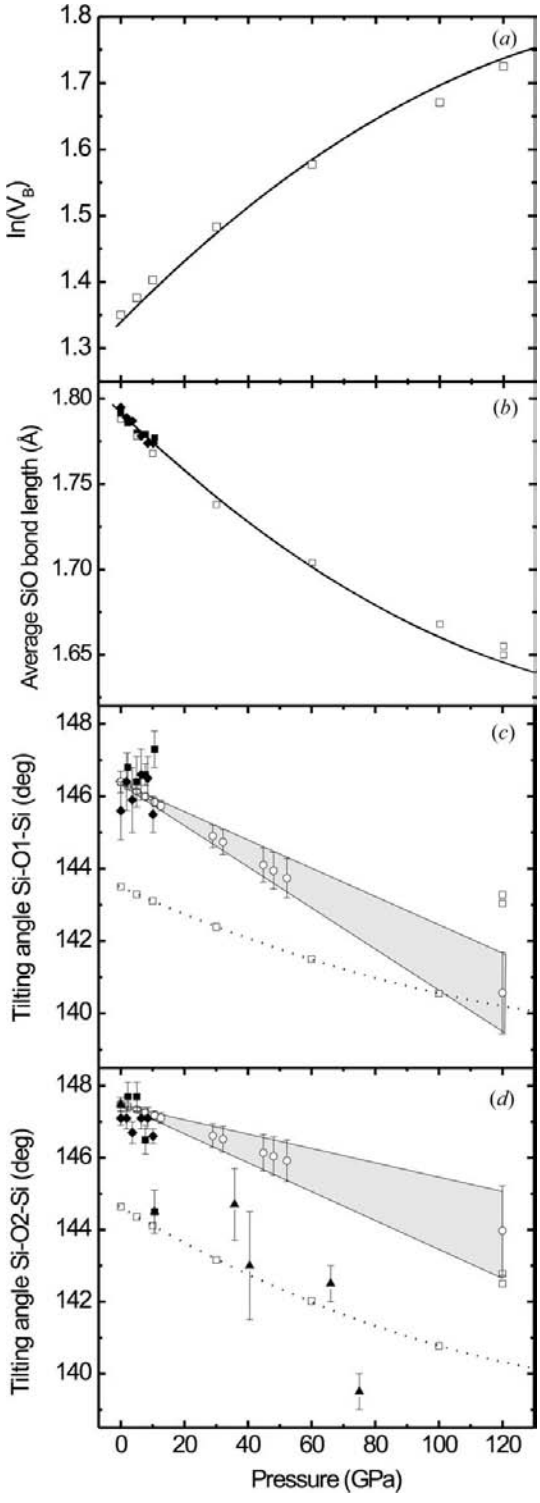

Figure 4
Comparison of the structure of $MgSiO_3$ at high pressures predicted by the *fixed coordinate* model (solid lines) with experimental data and *ab initio* computer simulations (open symbols: Wentzcovitch *et al.*, 1995; Iitaka *et al.*, 2004; Tsuchiya *et al.*, 2004). Solid symbols represent experimental data (square: Ross & Hazen, 1990; diamond: Vanpeteghem *et al.*, 2006; triangle: Fiquet *et al.*, 2000).

4. Summary

We have developed a method based upon the principle of bond-valence matching between the polyhedra in perovskites to predict the evolution of perovskite structures at high pressures, based only upon knowledge of the room-pressure structure and the unit-cell parameters at high pressures. In addition, as part of this analysis we have shown that it is possible to consider the evolution of the structures of $GdFeO_3$-type perovskites at high pressure to be effectively equal to the sum of two components. One is the compression of the structure through reduction of the unit-cell parameters, while the fractional coordinates of the atoms remain fixed. Within this component, all of the volume elements within the unit cell undergo the same fractional volume compression and thus have the same volume compressibilities. We have also found that because the observed compression of the unit-cell parameters of *Pbnm* perovskites is usually approximately isotropic, this component of compression does not result in significant change in the tilts of the octahedra. Therefore, the observed pressure-induced tilting of the octahedra in perovskites arises from our second component of compression that comprises changes in the fractional coordinates of the atoms. This analysis has allowed us to derive reliable predictions of the average linear compressibility of the A—O bonds within the perovskite structure from estimates of the compressibility of the B—O bonds.

The principle of bond-valence matching that underlies these calculations has already been shown to be applicable to perovskites in general (*e.g.* Angel, Zhao & Ross, 2005; Angel, Ross & Zhao, 2005; Zhao *et al.*, 2004*c*). Thus, the evolution of perovskites with other tilt systems and space-group symmetries should be equally well predicted by the method we have described here. It is also clear that the principle of bond-valence matching also applies, at least qualitatively, to other framework structures (*e.g.* Angel, Zhao & Ross, 2005). As extreme examples, both the ReO_3 and $BB'(OH)_6$ structure types possess the same octahedral frameworks as the perovskite, but without any extra-framework cation in the A site. This suggests that the site parameter M_A for these perovskites is equal to zero and thus implies that β_B is close to

zero, according to the relation $\beta_B/\beta_A = M_A/M_B$ and that these structures should exhibit increased tilting with increasing pressure. These predictions appear to be confirmed by recent high-pressure experiments (Jørgensen *et al.*, 2004; J. Zhao *et al.* unpublished). We also observe that the compression of minerals composed of other frameworks of corner-linked AlO_4 and SiO_4 tetrahedra is accompanied by increased tilting of almost rigid tetrahedra and significant compression of the bonds to the extra-framework cations. Similar behavior is observed for some framework structures composed of both tetrahedra and octahedra. In principle, therefore, the methods developed here for predicting the high-pressure behavior of perovskites should be adaptable to a wide range of framework structures.

The authors acknowledge with gratitude the financial support for this work derived from NSF grant EAR- 0408460 and Virginia Tech. We thank Fabrizio Nestola and Carine Vanpeteghem of Virginia Tech for useful discussions.

References

Allan, N. L. (2004). *Chemical Thermodynamics of Materials: Macroscopic and Microscopic Aspects. Svein Stølen and Tor Grande.* New York: John Wiley and Sons, Ltd.

Angel, R. J., Ross, N. L. & Zhao, J. (2005). *Eur. J. Mineral.* **17**, 193–199.

Angel, R. J., Zhao, J. & Ross, N, L. (2005). *Phys. Rev. Lett.* **95**, 025503-1.

Baerlocher, Ch., Hepp, A. & Meier, W. M. (1976). *DLS*-76; http://olivine.ethz.ch/LFK/software/xrs/dls76.html. Institute of Crystallography, Switzerland.

Berkowski, M., Fink-Finowicki, J., Piekarczyk, W., Perchuć, L., Byszewski, P., Vasylechko, L. O., Savytskij, D. I., Mazur, K., Sass, J., Kowalska, E. & Kapuśniak, J. (2000). *J. Cryst. Growth*, **209**, 75–80.

Brese, N. E. & O'Keeffe, M. (1991). *Acta Cryst.* B**47**, 192–197.

Brodholt, J. P., Oganov, A. R. & Price, G. D. (2002). *Philos. Trans. R. Soc. London A*, **360**, 2507–2520.

Brown, I. D. (1992). *Acta Cryst.* B**48**, 553–572.

Brown, I. D. (2001). *The Chemical Bond in Inorganic Chemistry. The Bond Valence Model.* Oxford University Press.

Brown, I. D. & Altermatt, D. (1985). *Acta Cryst.* B**41**, 244–247.

Fiquet, G., Dewaele, A., Andrault, D., Kunz, M. & Le Bihan, T. (2000). *Geophys. Res. Lett.* **27**, 21–24.

Glazer, A. M. (1972). *Acta Cryst.* B**28**, 3384–3392.

Hazen, R. M. & Finger, L. W. (1979). *J. Geophys. Res.* **84**, 6723–6728.

Howard, C. J. & Stokes, H.T. (2005). *Acta Cryst.* A**61**, 93–111.

Iitaka, T., Hirose, K., Kawamura, K. & Murakami, M. (2005). *Nature*, **430**, 442–445.

Jørgensen, J.-E., Marshall, W. G., Smith, R. I., Staun Olsen, J. & Gerward, L. (2004). *J. Appl. Cryst.* **37**, 857–861.

Koopmans, H. J. A., van de Velde, G. M. H. & Gellings, P. J. (1983). *Acta Cryst.* C**39**, 1323–1325.

Kung, J., Angel, R. J. & Ross, N. L. (2001). *Phys. Chem. Miner.* **28**, 35–43.

Liu, H.-Z, Chen, J., Hu, J., Martin, C. D., Weidner, D. J., Häusermann, D. & Mao, H.-K. (2005). *Geophys. Res. Lett.* **32**, L040304.

Lufaso, M. W. & Woodward, P. M. (2001). *Acta Cryst.* B**57**, 725–738.

Magyari-Köpe, B., Vitos, L., Grimvall, G., Johansson, B. & Kollár, J. (2002). *Phys. Rev. B*, **65**, 193107–193111.

Megaw, H. D. (1973). *Crystal Structures – a Working Approach.* Philadelphia: W. B. Saunders.

Payne, M. C., Teter, M. P., Allan, D. C., Arias, T. A. & Joannopoulos, J. D. (1992). *Rev. Mod. Phys.* **64**, 1045–1097.

Rao, G. H., Bärner, K. & Brown, I. D. (1998). *J. Phys. Condens. Matter*, **10**, L757–L763.

Ross, N. L. (1998). *Phys. Chem. Miner.* **25**, 597–602.

Ross, N. L. & Angel, R. J. (1999). *Am. Mineral.* **84**, 277–281.

Ross, N. L. & Chaplin, T. D. (2003). *J. Solid State Chem.* **172**, 123–126.

Ross, N. L. & Hazen, R. M. (1990). *Phys. Chem. Miner.* **17**, 228–237.

Ross, N. L., Zhao, J. & Angel, R. J. (2004*a*). *J. Solid State Chem.* **177**, 1276–1284.

Ross, N. L., Zhao, J. & Angel, R. J. (2004*b*). *J. Solid State Chem.* **177**, 3768–3775.

Ross, N. L., Zhao, J., Burt, J. B. & Chaplin, T. D. (2004). *J. Phys. Condens. Matter*, **16**, 5721–5730.

Salinas-Sanchez, A., Garcia-Muñoz, J. L., Rodriguez-Carvajal, J., Saez-Puche, R. & Martinez, J. L. (1992). *J. Solid State Chem.* **100**, 201–211.

Sasaki, S., Prewitt, C. T., Bass, J. D. & Schulze, W. A. (1987). *Acta Cryst.* C**43**, 1668–1674.

Sasaki, S., Prewitt, C. T. & Liebermann, R. C. (1983). *Am. Mineral.* **68**, 1189–1198.

Takemura, K. (2001). *J. Appl. Phys.* **89**, 662–668.

Thomas, N. W. (1989). *Acta Cryst.* B**45**, 337–344.

Tsuchiya, T., Tsuchiya, J., Umemoto, K. & Wentzcovitch, R. M. (2004). *Earth Planet. Sci. Lett.* **224**, 241–248.

Wentzcovitch, R. M., Karki, B. B., Cococcioni, M. & de Gironcoli, S. (2004). *Phys. Rev. Lett.* **92**, 018501–1.

Wentzcovitch, R. M., Ross, N. L. & Price, G. D. (1995). *Phys. Earth Planet. Int.* **90**, 101–112.

Woodward, P. M. (1997*a*). *Acta Cryst.* B**53**, 32–43.

Woodward, P. M. (1997*b*). *Acta Cryst.* B**53**, 44–66.

Vanpeteghem, C. B., Zhao, J., Angel, R. J., Ross, N. L. & Bolfan-Casanova, N. (2006). *Geophys. Res. Lett.* **3**, L03306.

Zhao, J., Ross, N. L. & Angel R. J. (2004*a*). *Phys. Chem. Miner.* **31**, 299–305.

Zhao, J., Ross, N. L. & Angel, R. J. (2004*b*). *Acta Cryst.* B**60**, 263–271.

Zhao, J., Ross, N. L. & Angel, R. J. (2004*c*). *J. Phys. Condens. Matter*, **16**, 8763–8773.

Zhou, J.-S., Goodenough, J. B. & Dabrowski, B. (2005). *Phys. Rev. Lett.* **94**, 226602.